SENSITIVITY ANALYSIS OF SMAP-REFLECTOMETRY (SMAP-R) SIGNALS TO VEGETATION WATER CONTENT

Nereida Rodriguez-Alvarez, Sidharth Misra, Mary Morris

Jet Propulsion Laboratory, California Institute of Technology, Pasadena, CA 91109

ABSTRACT

Global Navigation Satellite System – Reflectometry (GNSS-R) techniques have proven successful to retrieve several geophysical parameters such as, ocean wind speed, soil moisture, altimetry, wetland dynamics, snow depth estimations. In this paper, the L2C GPS signals measured from the Soil Moisture Active Passive (SMAP) radar after its malfunction is used to investigate the effect of the vegetation water content on the electromagnetic signal. The SMAP-Reflectometry (SMAP-R) measurements are obtained at V and H polarizations allowing for not only signal-to-noise ratio (SNR) analysis but also for polarimetric ratio (PR) studies.

Index Terms— SMAP, reflectometry, GNSS-R, vegetation water content, polarimetry

1. INTRODUCTION

The use of Global Navigation Satellite System – Reflectometry (GNSS-R) techniques in remote sensing has grown exponentially for the past few decades. A number of studies have used these techniques over the ocean to retrieve altimetry and sea state information [1-7], over land to retrieve soil moisture [8-14], and over the ice to retrieve altimetry and ice age [15,16]. With the launch of TechDemosSat-1 (TDS-1) [17] and Cyclone Global Navigation Satellite Signals (CYGNSS) [18, 19] the studies have multiplied. Both, TDS-1 and CYGNSS have allowed better ocean wind studies [20-22] and have make possible land surface studies. On one hand, CYGNSS with its increased temporal and spatial resolution, has made possible studies on soil moisture [23] or wetlands dynamics [24-27] from the space. On the other hand, TDS-1, with its polar coverage, has benefited studies of polar sea ice, in terms of altimetry [28], sea ice detection [29], sea ice concentration [30] and sea ice type [31]. The Soil Moisture Active Passive (SMAP) radar instrument malfunction opened the door to a new set of measurements. The radar was switched to 1227.45 MHz to collect GPS L2C signals on August 20, 2015. The characteristics of these measurements differ from the current available from missions like TDS-1 or CYGNSS in terms of polarization (H and V instead of LHCP), high antenna gain (36 dB) and narrow footprint (40 km diameter).

In this work, the SMAP-R measurements are used to study the effect of the vegetation water content on the bistatic radar signals. The selected area under study is the US Midwest between 30 N and 40 N degrees latitude and 105 W and 80 W degrees longitude. The impact of the vegetation water content is analyzed seasonally considering the different land covers and the soil moisture underneath the vegetation canopy. There is a previous study [32] that uses the SMAP-R signal at a broad resolution, spatially averaging the information at 1-degree lat/lon boxes, to assess polarimetric studies of the land and the cryosphere. Section 2 defines the specifics of the SMAP-R measurements, section 3 describes the main parameters affecting the SMAP-R signal over land and section 4 describes the results for the preliminary qualitative analysis. We expect this analysis to be quantitative by the IGARSS 2019 conference timeframe.

2. SMAP-R MEASUREMENT CHARACTERISTICS

The I/Q samples received at the SMAP radar working in receiver mode are publicly available at the Earthdata website (https://earthdata.nasa.gov). The data is filtered for those geometries where there is potential to capture a specular point. Those selected I/Q samples are post-processed into delay-Doppler maps (DDM) [33, 34], with a 5 ms coherent time and 25 ms incoherent time (5 incoherent summations). The SMAP antenna points to a fixed 40 degrees incidence angle. The SMAP beamwidth antenna allows to capture reflections at +/- 3 degrees from the central 40 degrees incidence angle. Observations are minimally affected by the variation in the incidence angle, mainly in scenarios where the signal is predominantly coherent. For example, the size of the first Fresnel zone for surfaces with very low roughness as croplands or wetlands, rivers or lakes is something in between [880 m x 1290 m] and [928 m x 1450 m], for 37.5 and 42.5 deg. incidence angle, respectively. For ocean surfaces, the scattering area is hundreds of kilometers and the assumption needs to be revised. SMAP has a high receiver gain: peak antenna gain is 36 dB at 40 deg. and the -3 dB beam width is 2.7 deg. Since antenna is rotating consecutive specular points are ~ 25 km apart. Transmitter gain is assumed to be constant since the geometry is fixed. Transmitted power is unknown, but the impact of its variations is assumed to be under 1.8 dB [35]. The observables derived from the DDMs used in this study are corrected signal-to-noise (SNR) measured at V and

H polarizations and the polarimetric ratio (PR), and are shown in figure 1. The corrected SNR corresponds to the measured SNR corrected for the path losses and the receiver gain.

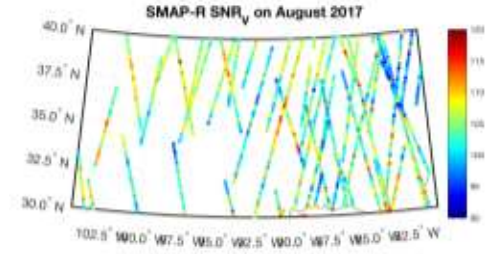

(a)

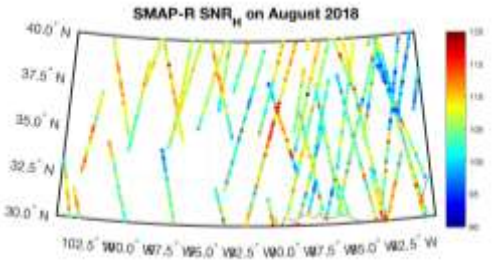

(b)

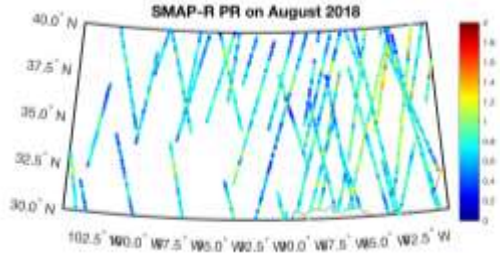

(c)

Figure 1. SMAP-R observables, (a) SNR H-pol, (b) SNR V-pol and (c) PR, measured over the US Midwest on August 2018.

3. THE BISTATIC SIGNAL OVER LAND

There are a number of parameters affecting the GPS signals as those go through the vegetation layer, impinge over the soil surface and reflect to the SMAP-R antenna after crossing the vegetation layer on their way up. Those parameters are the vegetation water content, the soil moisture, the soil roughness and the topography. Figure 2 shows the digital elevation model (DEM) map for the area under study.

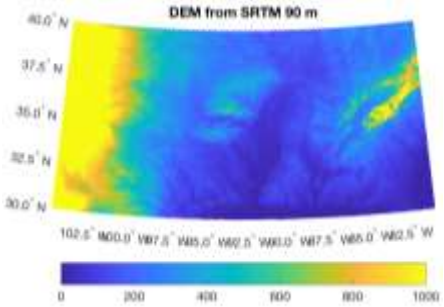

Figure 2. DEM of the area under study, scale in meters.

This map has been obtained from the Shuttle Radar Topography Mission (SRTM) 90 m DEM product. The SMAP-R signals show differences under different topography conditions, but those differences do not vary seasonally. By analyzing changes in a particular area over time, we can assume topography to be invariant. In addition, we should use areas where the topography remains nearly constant. Next, Figure 3 shows the soil moisture (SM) map from the SMAP Level 3 SM product enhanced (SPL3SMP_E, [36]) for the area under study.

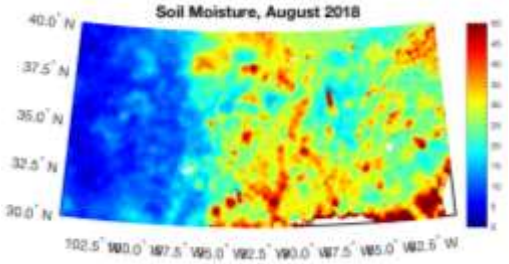

Figure 3. SM map of the area under study, scale in %.

The SMAP-R H and V signals are affected by soil moisture. The more water content in the soil the strongest the reflection. We will start with the SM product derived from SMAP radiometer [36] but other sources may as well be considered. We will take the SM product as an ancillary dataset to analyze areas with similar soil moisture content together helping to distinguish between vegetation effects and soil moisture effects. In other words, we will proceed by filtering by soil moisture levels and then analyzing the impact of vegetation water content (VWC) alone. Particularly it is important to consider this in agricultural areas where soil moisture varies seasonally. Figure 4 shows an example of the VWC maps used as the reference in this study.

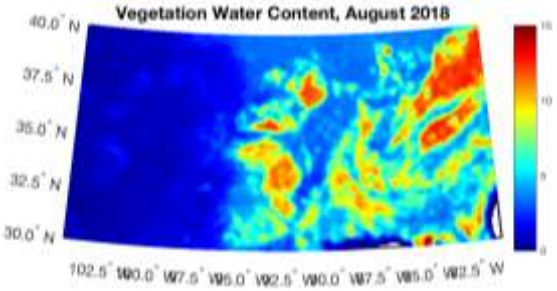

Figure 4. VWC map of the area under study, scale in kg/m^2.

Those maps are part of the ancillary data [37] from SMAP soil moisture algorithm, [36]. The VWC is provided in the SMAP dataset and follows the method explained in [38]. This method provides a VWC estimation incorporating foliage and stem water content. First, estimates the water content of the foliage based on a Normalized Difference Vegetation Index (NDVI) approach. Then, estimates the stem water content through observations and Leaf Area Index (LAI) modeled by NDVI. Land cover types are considered using the MODIS

(MCD12Q1) International Geosphere-Biosphere Programme (IGBP) classification scheme [38]. The SMAP-R H and V signals are affected by vegetation. The vegetation layer attenuates the SNR signal, the more water content on the vegetation the more attenuation the signal suffers. Also, vegetation water content varies seasonally.

4. QUALITATIVE ANALYSIS OF THE VWC EFFECTS ON THE SMAP-R SIGNAL

In order to understand the impact of the vegetation water content on the SMAP-R signals, we will analyze the effects on the SNR at V pol in two different ways:

- an analysis of VWC differences observed over similar land covers, and
- the possibility of monitoring seasonal variations observed at the same locations.

For the first analysis, we have selected different areas with constant land types obtained from MODIS land cover maps: croplands and deciduous broadleaf forest.

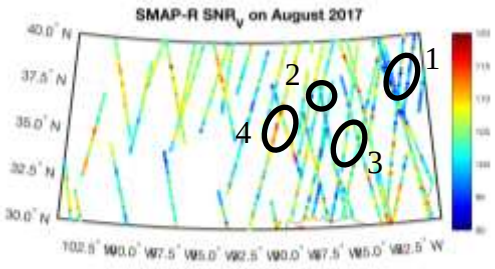

Figure 5. Areas selected in this SNR$_V$ correspond to areas with very different VWC values in figure 4. Scale in dB.

Comparing to the VWC in figure 4, we see that the higher the VWC value the lower the SNR. Summarized in Table 1.

Table 1. Summary of mean VWC values from figure 4 and SNR$_V$ values at the circled areas.

Area	VWC (kg/m^2)	SNR (dB)
1	12	95
2	10	100
3	7.5	105
4	4	112

For the second analysis we have initially focused in a cropland area, marked in figure 6. Important characteristics of this areas are:

- soil moisture, due to irrigation of crops, would be considerably higher in summer than in winter: SM increase implies SNR$_V$ increase.
- VWC is higher in summer when crops are present than winter: VWC increase implies SNR$_V$ decrease.
- there is a river in the circled area: river in the SMAP footprint implies SNR$_V$ increase.

With this being said, the selected area shows a big change in vegetation water content, as it is show in figure 6, between January 2018 and August 2018.

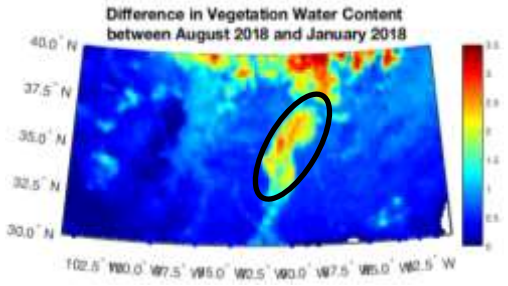

Figure 6. VWC differences observed between January 2018 (winter) and August 2018 (summer).

An increase of 2 kg/m^2 from January to August 2018 causes ~ a decrease in the SNR$_V$ of 6 dB. So, this would indicate that the attenuation suffered from the increase in vegetation water content is stronger than the increase in SNR caused by the increase in SM. Further and quantitative analysis will be presented at the conference, showing the impact of the VWC on the SNR at both polarizations and on the PR.

5. CONCLUSIONS

This paper describes the preliminary analysis of the impact of VWC in the GPS signal measured at the SMAP radar in bistatic configuration, SMAP-R. The higher the VWC the lower the SNR. If we can quantify the impact of the VWC under a controlled scenario, i.e. adding layers of information regarding, the roughness, topography, soil moisture and type of land cover, next steps will go in the direction of creating a retrieval algorithm based on the most sensitive GNSS-R observables. Using this information derived from SMAP-R signals will help filling the gaps in other instruments and/or creating an independent source of VWC information.

6. ACKNOWLEDGEMENT

This research was carried out at the Jet Propulsion Laboratory, California Institute of Technology, under a contract with the National Aeronautics and Space Administration. In particular, the research on the sensitivity of SMAP-R signals to vegetation water content was supported by the JPL fund on R&A Hydrology & Weather from the Soil Moisture Active Passive (SMAP) project. © 2018. California Institute of Technology. Government sponsorship acknowledged.

7. REFERENCES

[1] M. Martín-Neira, "A Passive Reflectometry and Interferometry System (PARIS): Application to Ocean Altimetry." ESA Journal, vol. 17. pp 331-355, 1993

[2] M. Martin-Neira, P. Colmenarejo, G. Ruffini, C. Serra, "Ocean Altimetry using the Carrier Phase of GNSS Reflected Signals," Proceedings of Ocean Winds 2000, Plouzane, France, CERSAT News, Issue 11, November 2000.

[3] Garrison, J., et al., "Wind speed measurements using forward scattered GPS signals." IEEE Trans. Geosci. Remote Sens., 40, 50–65, 2002.

[4] Clarizia, M. P., et al., "Analysis of GNSS-R delay-Doppler maps from the UK-DMC satellite over the ocean." Geophys. Res. Lett., 36, L02608, 2009.

[5] Marchan-Hernandez, J.F., et al., "Sea-state determination using GNSS-R data." IEEE Geosci. Remote Sens. Lett., 7, 621–625, 2010.

[6] Rodriguez-Alvarez, N., et al., "Airborne GNSS-R wind retrievals using delay-Doppler maps." IEEE Trans. Geosci. Remote Sens., 51, 626–641, 2013.

[7] Soulat, F., et al., "Sea state monitoring using coastal GNSS-R," Geophysical Research Letters, vol. 31, no. 21.pp

[8] D. Masters , "Surface Remote Sensing Applications of GNSS Bistatic Radar: Soil Moisture and Aircraft Altimetry," PhD dissertation, University of Colorado, 2004.

[9] D. Masters, et al., "GPS signal scattering from land for moisture content determination," Proceedings of the International Geoscience and Remote Sensing Symposium 2000, vol.7, pp. 3090-3092, Honolulu, USA.

[10] Egido, A., et al., "Soil moisture monitorization using GNSS reflected signals," in Proc. 1st Colloq. Sci. Fundam. Aspects Galileo Programme, Toulouse, France, Oct. 1–4, 2007.

[11] Grant, M. S., et al., "Terrain moisture clas- sification using GPS surface-reflected signals," IEEE Geosci. Remote Sens. Lett., vol. 4, no. 1, pp. 41–45, Jan. 2007.

[12] Rodriguez-Alvarez, N., et al., "Soil moisture retrieval using GNSS-R techniques: Experimental results over a bare soil field," IEEE Trans. Geosci. Remote Sens., 47(11), 3616–3624, 2009.

[13] Rodriguez-Alvarez, N., et al. "Land geophysical parameters retrieval using the interference pattern GNSS-R technique," IEEE Trans. Geosci. Remote Sens., 49(1), 71–84, 2011.

[14] Larson, K., et al., "Use of GPS receivers as a soil moisture network for water cycle studies," Geophys. Res. Lett., 35, L24405, 2008.

[15] Komjathy, A., et al., "Sea Ice Remote Sensing Using Surface Reflected GPS Signals," Proceedings of the International Geoscience and Remote Sensing Symposium 2000, Honolulu, USA.

[16] Semmling, A., et al. "Detection of arctic ocean tides using interfer- ometric GNSS-R signals," Geophys. Res. Lett., 38, L04103, 2011.

[17] Unwin, M., et al., "Spaceborne GNSS-Reflectometry TechDemoSat-1: Early Mission Operations and Exploitation." IEEE J. Sel. Top. Appl. Earth Obs. Remote Sens., 9, 4525–4539, 2016.

[18] Ruf, C.S., et al., "The CYGNSS nanosatellite constellation hurricane mission," in 2012 IEEE International Geoscience and Remote Sensing Symposium. IEEE, pp. 214–216, 2012.

[19] Ruf, C., et al., "CYGNSS: Enabling the Future of Hurricane Prediction [Remote Sensing Satellites]," IEEE Geoscience and Remote Sensing Magazine, vol. 1, no. 2, pp. 52–67, 2013.

[20] Foti, G., et al., "Spaceborne GNSS reflectometry for ocean winds: First results from the UK TechDemoSat-1 mission". Geophys. Res. Lett., 42, 5435-5441, 2015.

[21] Clarizia, M.P., et al., "First spaceborne observation of sea surface height using GPS-Reflectometry". Geophys. Res. Lett., 43, 767-774, 2016.

[22] Clarizia, M. P., and C. S. Ruf, "Wind Speed Retrieval Algorithm for the Cyclone Global Navigation Satellite System (CYGNSS) Mission," IEEE Trans Geosci. Remote Sens., doi:10.1109/TGRS.2016.2541343, 2016.

[23] Chew, C. C., and Small, E. E. "Soil moisture sensing using spaceborne GNSS reflections: Comparison of CYGNSS reflectivity to SMAP soil moisture." Geophysical Research Letters, 45, 4049–4057.

[24] Nghiem, S. V., et al., "Wetland monitoring with global navigation satellite system reflectometry", Earth and Space Science, 2016, vol. 4, no. 1, pp. 16–39.

[25] Zuffada, C., et al., Global navigation satellite system reflectometry (GNSS-R) algorithms for wetland observations, in 2017 IEEE International Geoscience and Remote Sensing Symposium (IGARSS), 2017, pp. 1126–1129.

[26] Jensen, K.; et al., "Assessing L-Band GNSS-Reflectometry and Imaging Radar for Detecting Sub-Canopy Inundation Dynamics in a Tropical Wetlands Complex." Remote Sens. 2018, 10, 1431.

[27] N. Rodriguez-Alvarez, et al., "Characterizing Wetland Inundation with GNSS-R", MDPI Remote Sensing, (in review)

[28] Li, W.; et al., "First spaceborne phase altimetry over sea ice using TechDemoSat-1 GNSS-R signals." Geophys. Res. Lett. 2017, 44, 8369-8376

[29] Yan, Q. and Huang, W. "Spaceborne GNSS-R sea ice detection using delay-doppler maps: First results from the U.K. TechDemoSat-1 mission." IEEE J. Sel. Top. Appl. Earth Obs. Remote Sens. 2016, 9, 10, 4795-4801.

[30] Alonso-Arroyo, A.; et al., "Sea Ice Detection Using U.K. TDS-1 GNSS-R Data". IEEE TGRS 2017, 55, 9, 4989-5001.

[31] N. Rodriguez-Alvarez, et al., "Arctic sea ice multi-step classification based on GNSS-R data from the TDS-1 mission". Remote Sensing of the Environment, (in review)

[32] Carreno-Luengo, H., et al.; "Spaceborne GNSS-R from the SMAP mission: First assessment of polarimetric scatterometry." 4095-4098, 2017.

[33] Zavorotny, V.U. and Voronovich, A.G; Scattering of GPS signals from the ocean with wind remote sensing application. IEEE TGRS. 2000, 38, 2, 951–964. doi:10.1002/2017GL074513.

[34] Voronovich, A.G and Zavorotny, V.U.; Bistatic radar equation for signals of opportunity revisited. IEEE TGRS. 2018, 56, 4, 1959-1968.

[35] Chew, C., et al., "SMAP radar receiver measures land surface freeze/thaw state through capture of forward-scattered L-band signals", Remote Sensing of Environment, Volume 198, Pages 333-344, 2017.

[36] O'Neill, P., et al., "Algorithm Theoretical Basis Document Level 2 & 3 Soil Moisture (Passive) Data Products". JPL D-66480. June 6, 2018. Available online at: https://smap.jpl.nasa.gov/documents/.

[37] Chan, S., et al., "Ancillary Data Report: Vegetation Water Content". JPL D-53061. January 21, 2013. Available online at: https://smap.jpl.nasa.gov/documents/.

[38] Hunt, e. R., et al.; "Global net carbon exchange and intra-annual atmospheric CO_2 concentrations predicted by an ecosystem process model and three-dimensional atmospheric transport model.", Global Biochemical Cycles, 10, 431-456, 1996.